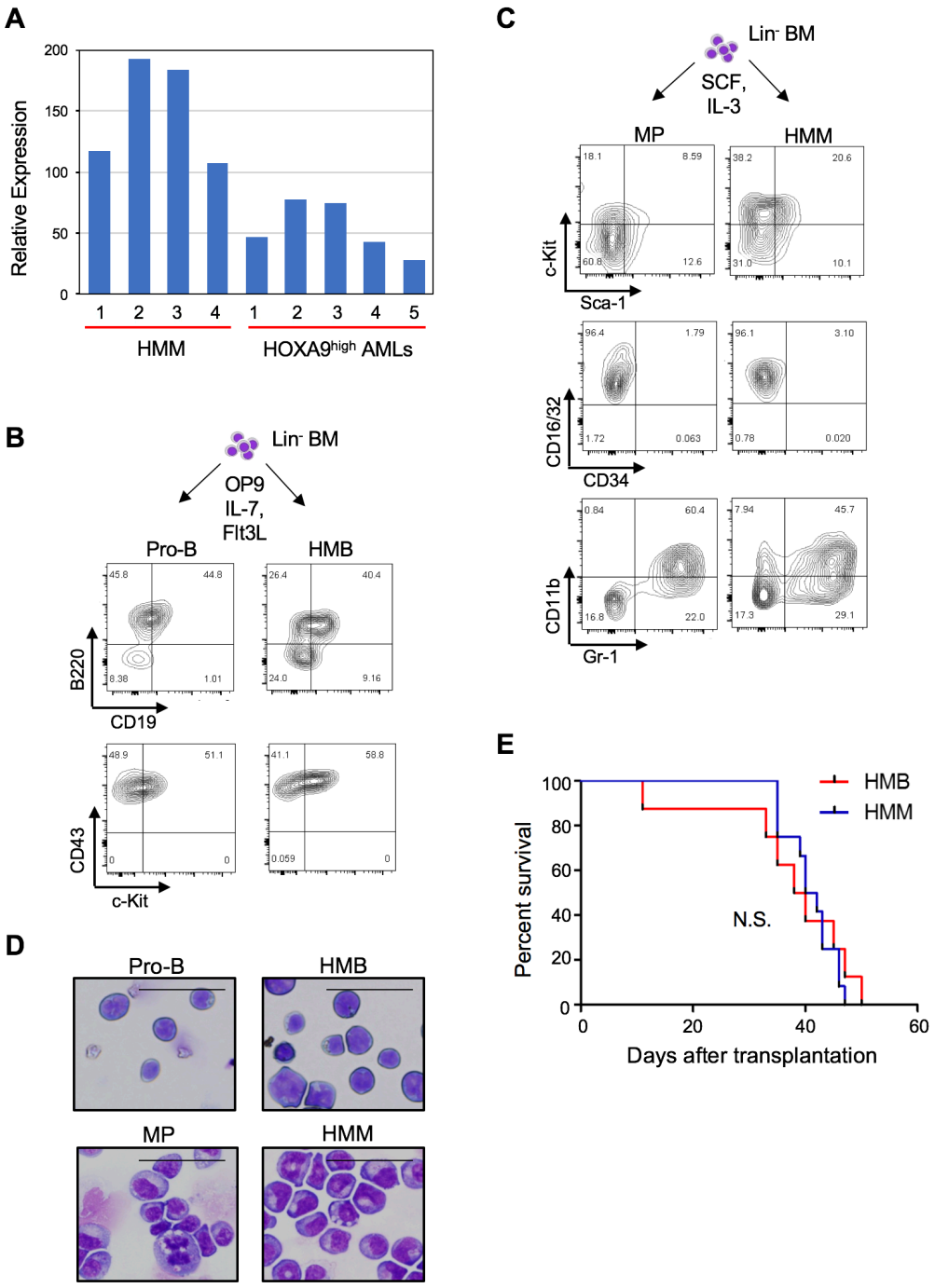

Figure S1, related to Figure 1. Establishment of HOXA9/MEIS1 leukemia cell lines. (A) Relative expression for *HOXA9* in HMM cells and human HOXA9^{high} AMLs. RPKM from RNA-seq was normalized against *GAPDH* and then against HOXA9 expression in control HSCs, which was arbitrarily set as 1. **(B)** Flow cytometric analysis of HMB and pro-B cells for pro-B surface markers CD19, B220, c-Kit and CD43. **(C)** Flow cytometric analysis of HMM and MP cells for myeloid surface markers c-Kit, Sca-1, CD16/32, CD34, CD11b and Gr-1. **(D)** Cytospin images of transformed HMB and HMM cells. Scale bar: 50 μm. **(E)** Survival curve of mice transplanted with HMM and HMB cells, which succumbed to acute leukemia around day 40.

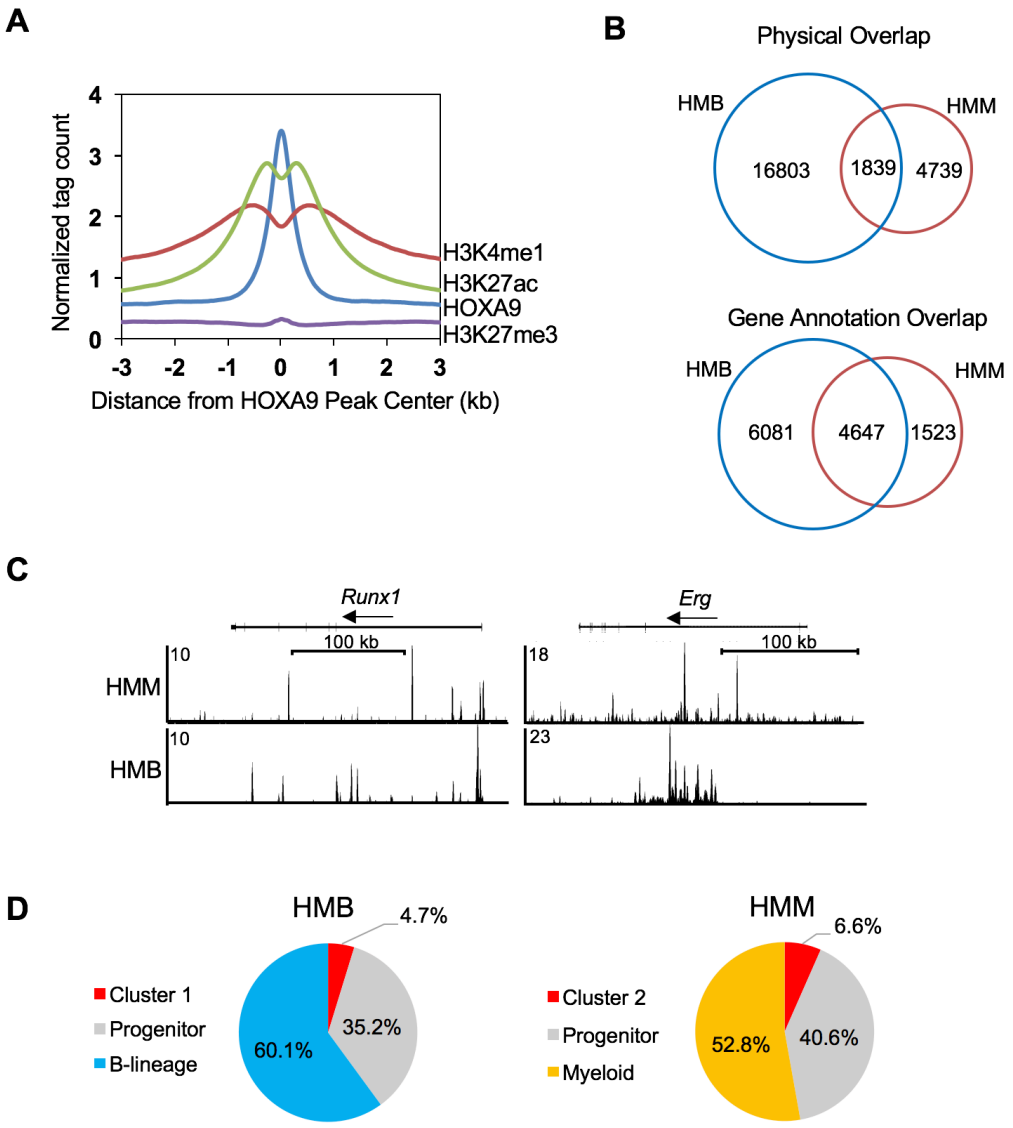

Figure S2, related to Figure 1 and 2. Genome-wide analysis of HOXA9 binding in HMM and HMB cells. (A) Composite plot showing average per base pair density of HOXA9, H3K4me1, H3K27ac and H3K27me3 at HOXA9 binding sites in HMB cells. Library size was normalized to 10^7 reads. **(B)** Venn diagram for physical and gene annotation overlaps of the HOXA9 binding sites in HMM and HMB cells. (**C)** UCSC browser views of HOXA9 peaks in close proximity to *Runx1* and *Erg* loci, showing the differential utilization of regulatory elements in different lineages. **(D)** Pie chart illustrating percentage of enhancers that were established in progenitors, lineage-committed cells or leukemia cells (cluster 1 and 2).

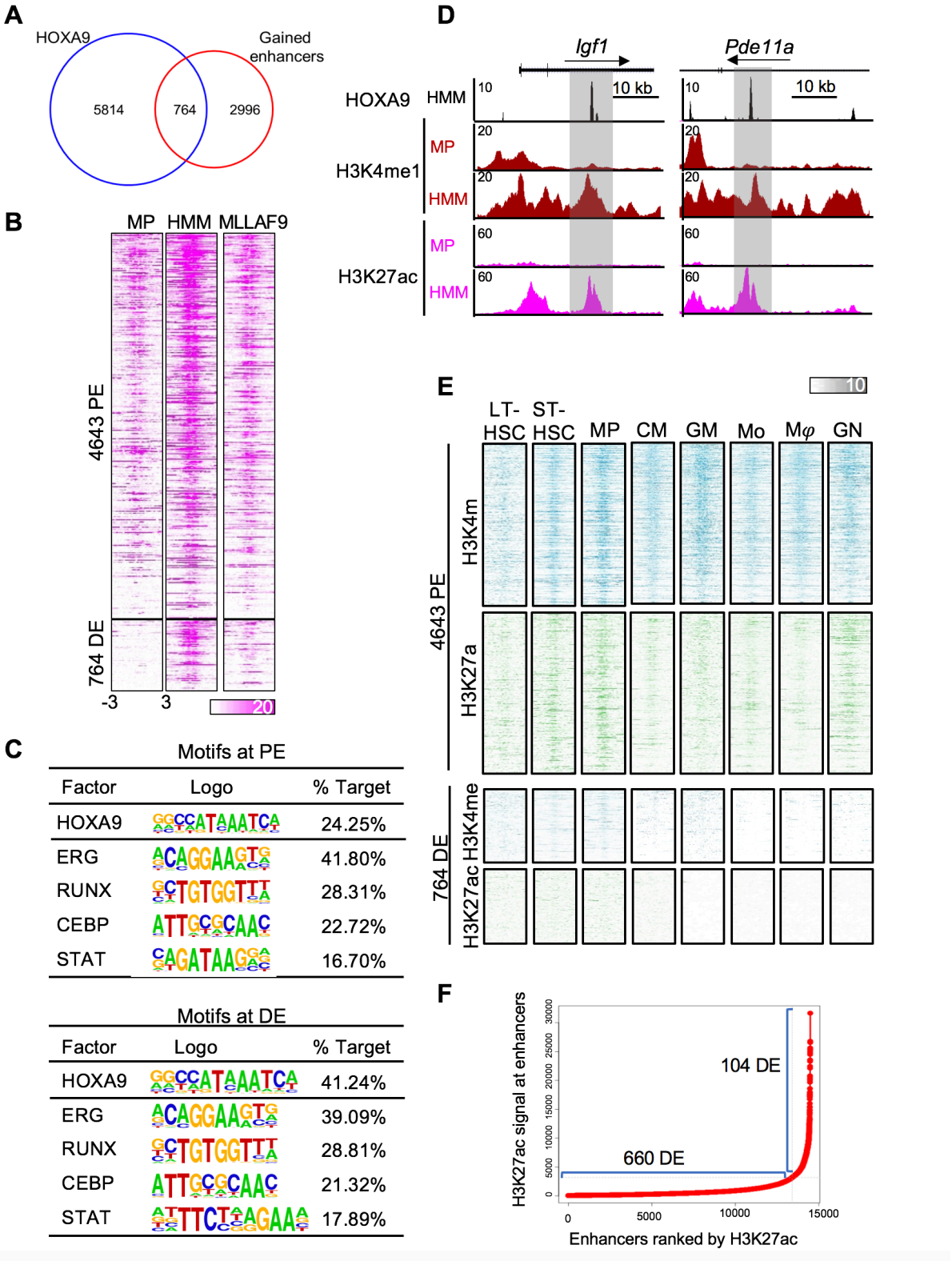

Figure S3, related to Figure 3. DE and PE analysis in HMM cells. (A) Venn diagram for overlap between HOXA9 binding sites and regions of gained H3K4me1 in HMM cells. **(B)** Heat map depicting H3K27ac signal at the 5,407 HOXA9-bound enhancers (4,643 PE and 764 DE) in MP, HMM and MLL-AF9 cells. Each row represents the 3 kb upstream and downstream region

centered on a HOXA9 peak. Peaks were sorted based on total normalized H3K4me1 tag counts in each category. **(C)** Motif analysis for HOXA9-bound PE and DE in HMM cells. **(D)** UCSC browser views for HOXA9, H3K4me1 and H3K27ac ChIP-seq data on two HOXA9-bound active enhancers annotated to *Igf1* and *Pde11a* loci. **(E)** Heat map for H3K4me1 and H3K27ac ChIP-seq signals at 4,643 PE and 764 DE in normal hematopoietic cell lineages as indicated on top. **(F)** Super enhancer analysis for 764 HOXA9-bound DE, which was based on H3K27ac density as previously described.

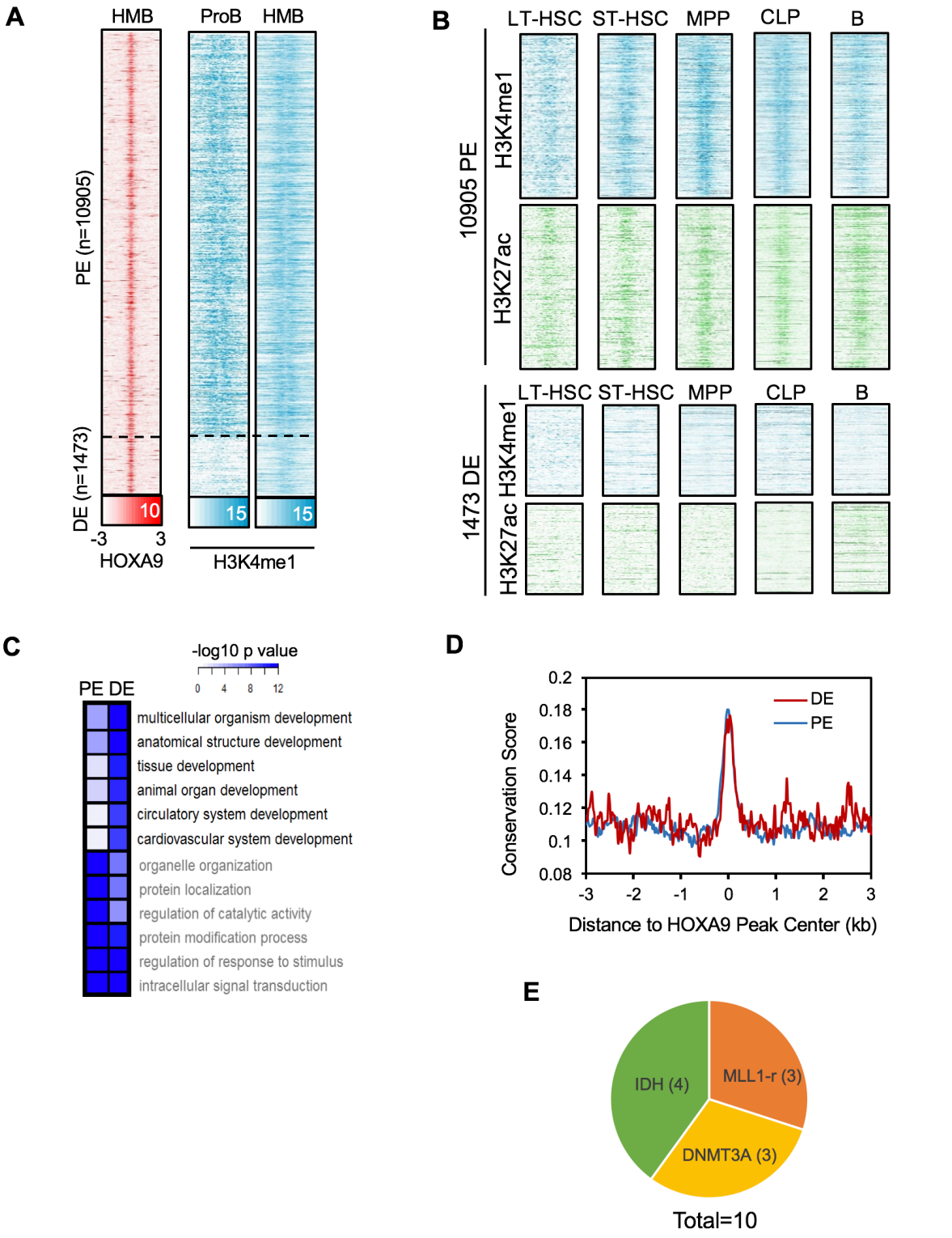

Figure S4, related to Figure 3. DE and PE in HMB cells. (A) Heat map of 12,389 HOXA9 peaks in HMB cells and corresponding H3K4me1 in HMB or Pro-B cells. Each row represents the 3 kb upstream and downstream region centered on a HOXA9 peak. Peaks were sorted based total normalized H3K4me1 tag counts in each category. **(B)** Heat map depicting signal

intensity of H3K4me1 at 10,905 PE and 1,473 DE in normal hematopoietic lineages as indicated on top. **(C)** Heat map for the Benjamini p-values of each PE and DE-associated GO term. **(D)** The conservation scores (Siepel et al., 2005) of the 6 kb regions centered on HOXA9 peaks in human AMLs. The regions were obtained after Liftover from murine DE (red) or PE (blue). **(E)** Known diagnostic mutations in 10 primary AML samples used in the study. MLL1-r, MLL1 rearranged leukemia.

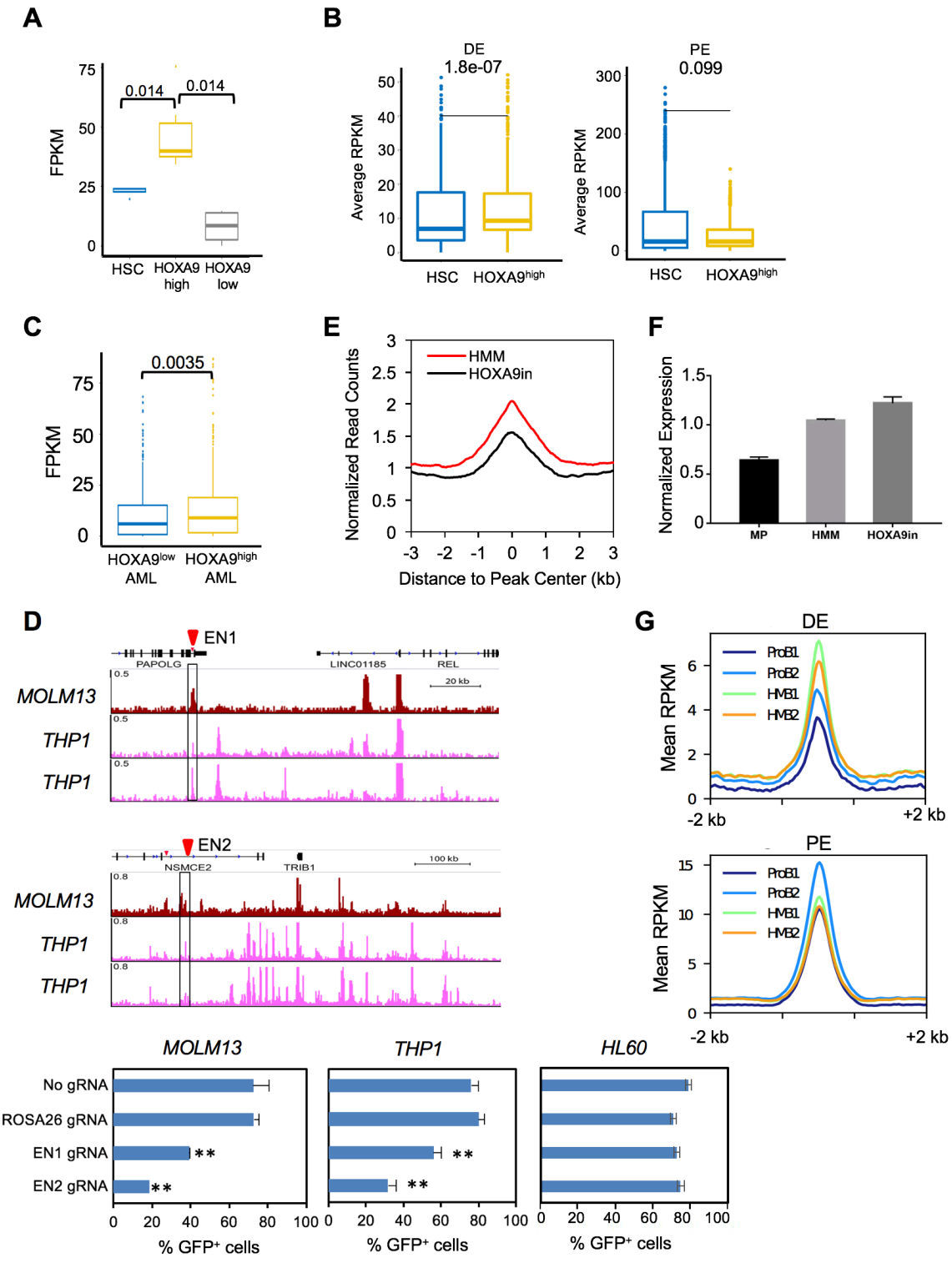

Figure S5, related to Figure 3 and 5. Enhancer analysis of human AML samples. (A) HOXA9 expression levels in normal hematopoietic progenitor cells (control) and six HOXA9^{high} and four HOXA9^{low} AML samples. **(B)** Normalized H3K4me1 read counts at DE and PE in HSC or primary human AMLs that have high HOXA9 expression. **(C)** FPKM values of genes

associated with DE in HOXA9^{high} and HOXA9^{low} samples as indicated. For **(A)-(C)**, p value was calculated from Mann-Whitney U test. The lower and upper edges of the box corresponded to the first and third quartiles (the 25th and 75th percentiles), respectively. The middle line represents the median value. **(D)** Top, UCSC browser view of H3K27ac at two enhancers EN1 and EN2 (red arrows), in human MOLM13 (Wan et al., 2017) and two independent THP1 cell lines (Phanstiel et al., 2017). Bottom, competitive co-culture assay showing negative selection of GFP^{+} human leukemia MOLM13, THP1 and HL60 cells (Barbieri et al., 2017) at day 7 after CRISPR–Cas9 mediated deletion of EN1 and EN2. Mean ± s.d. of three independent infections was presented. **(E)** Composite plot for normalized read count for H3K4me1 peaks at DE that were not bound by HOXA9 in HMM cells with or without HOXA9 inactivation. **(F)** *Cebpa* expression level (RPKM) in MP, HMM and HOXA9in cells. Mean of relative expression against *Gapdh* was presented, which was arbitrarily set as 1. Error bars represented standard deviation of three biological repeats. **(G)** Composite plot for ATAC-seq signals at the HOXA9-bound DE and PE in pro-B and HMB cells, respectively. HMB cells had higher levels of open chromatin at DE as compared to pro-B cells.

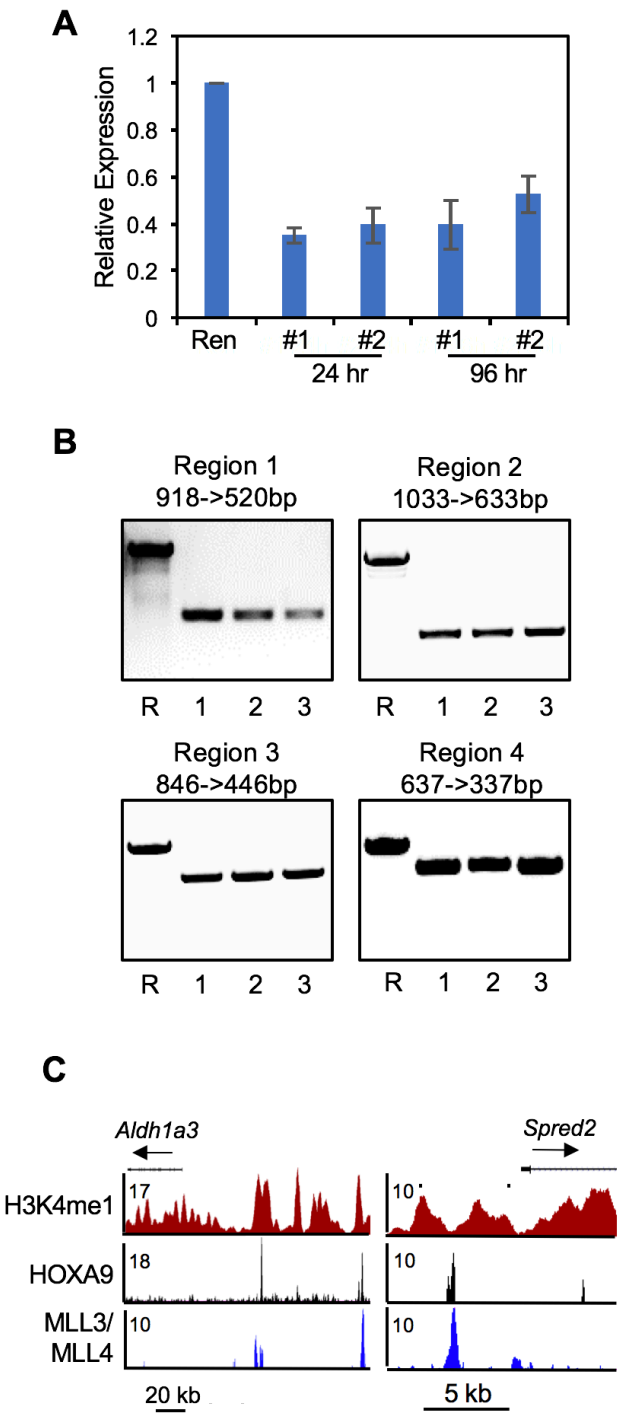

Figure S6, related to Figure 5 and 6. Loss of function studies at DE in HOXA9/MEIS1 leukemia (A) RT-PCR for *Aldh1a3* after 24 or 96 hours knock-down by two shRNAs. Mean of relative expression against control knockdown at 24 hours was presented, which was arbitrarily set as 1. Error bars represented standard deviation of three biological repeats. **(B)** Agarose gel images to demonstrate successful deletion of regions corresponding to regions 1-4 at *Aldh1a3* loci as indicated on top. **(C)** Representative ChIP-seq peaks for HOXA9, H3K4me1 and MLL3/4 at *Aldh1a3* and *Spred2* loci.

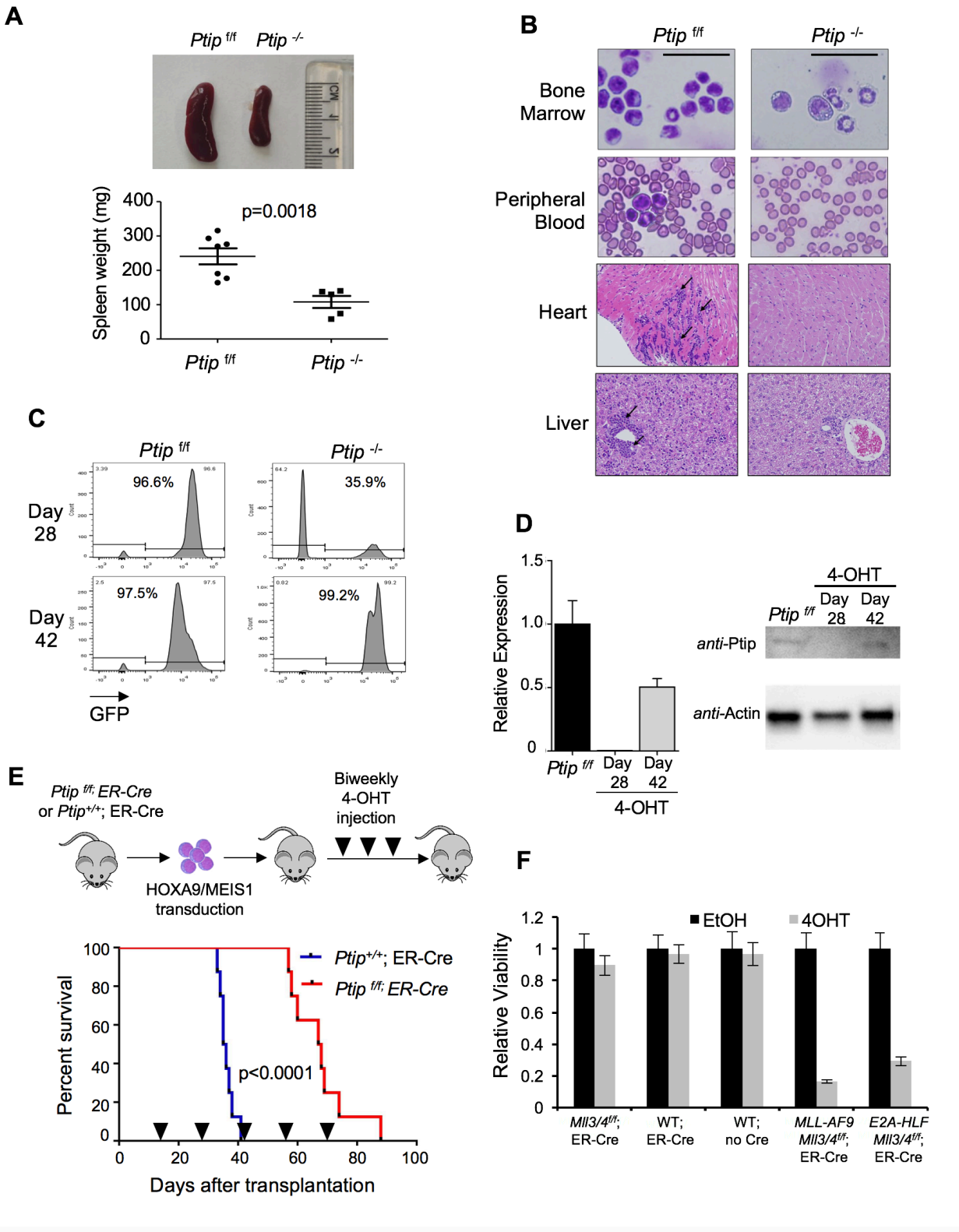

Figure S7, related to Figure 7. In vivo analysis of HOXA9/MEIS1 leukemogenesis. (A) Representative image of spleens from recipient mice Day 30 post transplantation. Bottom, spleen weights from two groups of mice as indicated on bottom. Average weights and standard

deviation (error) were presented. Statistical analysis was performed with p=0.0018. **(B)** Wright-Giemsa staining of peripheral blood smear and histology of organs (H&E staining) of recipient mice (as indicated on top) at Day 30 post transplantation. Scale bars: 50 μm. **(C)** Flow cytometric analysis for GFP^+ bone marrow cells at two time points, Day 28 and Day 42, after transplantation. **(D)** Quantitative RT-PCR and immunoblot for *Ptip* expression in HOXA9/MEIS1 *Ptip* $^{f/f}$; ER-Cre cells and cells analyzed by flow cytometry in C. For RT-PCR, average expression of *Ptip* was normalized against that of untreated *Ptip* $^{f/f}$; ER-Cre cells, which was arbitrarily set as 1. Error bars represented standard deviation of three biological repeats. **(E)** Top, transplantation scheme for leukemia maintenance study; Bottom, survival curve for mice recipients of *Ptip* $^{+/+}$; ER-CRE $^{+/-}$ or *Ptip* $^{f/f}$; ER-CRE $^{+/-}$ HOXA9/MEIS1 leukemia cells. The bi-weekly 4-OHT treatment was initiated at Day 14 via oral gavage as indicated by black arrows. $p<0.0001$, log-rank test. **(F)** Cell Titer Glo analysis for cell proliferation in cells as indicated on bottom. Average value after normalization against ethanol treated sample was presented, which was set as 1. Error bar represented standard deviation of three repeats.

Table S4, related to STAR Methods. Primers and gRNAs.

Gene/Genomic region	Sequence/Assay ID	Assay
Aldh1a3-VIEWPT-F	GGGTGGTTTCTTTCTGATAAGCT	4C-seq
Aldh1a3-VIEWPT-R	GGGTGGTTTCTTTCTGATAAGCT	4C-seq
Aldh1a3-1F	GATGTGGGGAGAGGTGAGAA	Gel electrophoresis
Aldh1a3-1R	GTCTCAGGCCTGTGGAAGAG	Gel electrophoresis
Aldh1a3-2F	ATGAGATTTGGCCTGCTCAC	Gel electrophoresis
Aldh1a3-2R	ACCCGACACAGTTGGAGTTC	Gel electrophoresis
Aldh1a3-3F	GCAGAGAAGGCACACAATCA	Gel electrophoresis
Aldh1a3-3R	CCCCAAACACCTACACCATC	Gel electrophoresis
Aldh1a3-4F	CTGTGTGTGCCTCTTGTGCT	Gel electrophoresis
Aldh1a3-4R	TCAGGGTTTTCGAAGCTGTT	Gel electrophoresis
Aldh1a3-1U2	CCTCCCATACACAAATGTAT	CRISPR gRNA
Aldh1a3-1D1	GCCATCCGTGAAATGTCAGC	CRISPR gRNA
Aldh1a3-2U1	TTTGTGTAGAAACAAAGACA	CRISPR gRNA
Aldh1a3-2D1	GTTTTATTTGGCACCTTACG	CRISPR gRNA
Aldh1a3-3U2	CACGCTCAAGCCCCAAACAT	CRISPR gRNA
Aldh1a3-3D1	GTGAACAAGAGATTGTGCCG	CRISPR gRNA
Aldh1a3-4U1	GTAATAATTGTGAGAAACGA	CRISPR gRNA
Aldh1a3-4D1	AGAGCAATCAAACTCAGATG	CRISPR gRNA
PAPOLG-1U2t	caccgTCAAGTGATTCGCCCGCCT	
PAPOLG -1U2b	aaacAGGCGGGCGAATCACTTGAc	
NSMCE2-1U1t	caccgATTAGCTAGGTGGCGTGGC	
NSMCE2-1U1b	aaacGCCACGCCACCTAGCTAATc	
*Aldh1a3*_-24k_F1	GGCTGCCAAGTTAACCCAA	ChIP
*Aldh1a3*_-24k_R1	GTCTCAGGCCTGTGGAAGAG	ChIP
*Aldh1a3*_49k_F2	GGGTGTTCACCACAACATGA	ChIP
*Aldh1a3*_49k_R2	GGAGCATCCTCTTAGCTGGTT	ChIP
*Aldh1a3*_77k_F1	GCTGCAAACTCCTGTTTGTTC	ChIP
*Aldh1a3*_77k_R1	GTGTCTGCCTACCACTCCCT	ChIP
*Aldh1a3*_118k_F1	TTAGGGAGCAATGGGAAGTG	ChIP
*Aldh1a3*_118k_R1	GGAACCACAGGGAGTTCTGA	ChIP
*Aldh1a3*_118k_F3	GGTGTCCTGTTTGTGCGTTC	ChIP
*Aldh1a3*_118k_R3	TCCAGGCCAGACCCTTAACT	ChIP
*Arid3a*_ChIP_F	GCGGGTTTGTCAAATATCTTC	ChIP
*Arid3a*_ChIP_R	GGAGTCGGTATTTCAAAGGC	ChIP
*Spred2*_ChIP_F	GGAGTTAAGAGGCAGGCAAC	ChIP
*Spred2*_ChIP_R	AGTTCCAGGCCAATTTGAAC	ChIP
*Stk10*_ChIP_F	GGAAAGCCGTAGGTCATGTT	ChIP
*Stk10*_ChIP_R	CCACCATCAACATCCACTTG	ChIP
Aldh1a3-exp-F	GGGTCACACTGGAGCTAGGA	RNA
Aldh1a3-exp-R	CTGGCCTCTTCTTGGCGAA	RNA
Gapdh-exp-F	AGGTCGGTGTGAACGGATTTG	RNA
Gapdh-exp-R	TGTAGACCATGTAGTTGAGGTCA	RNA
Actb-exp-F	GGCTGTATTCCCCTCCATCG	RNA
Actb-exp-R	CCAGTTGGTAACAATGCCATGT	RNA

*shmirAldh*1a3-1	GCAGATCAACAAGATAGCCTT	shRNA
*shmirAldh*1a3-2	CGAATCCAAGAGTGGAAGAAA	shRNA
Cebpd	Mm00786711_s1	Sigma RNA probe set
Jun	Mm00495062_s1	Sigma RNA probe set
Cebpg	Mm01266786_m1	Sigma RNA probe set
Dntt	Mm00493300_m1	Sigma RNA probe set
Fos	Mm00487425_m1	Sigma RNA probe set
Ebf1	Mm00432948_m1	Sigma RNA probe set
Pax5	Mm00435501_m1	Sigma RNA probe set
Rag1	Mm01270936_m1	Sigma RNA probe set
Cebpa	Mm00514283_s1	Sigma RNA probe set
Pparg	Mm01184322_m1	Sigma RNA probe set
Myc	Mm00487804_m1	Sigma RNA probe set
Gapdh	Mm99999915_g1	Sigma RNA probe set
Actb	Mm00607939_s1	Sigma RNA probe set